

## Influence of interstitially soluted iron on structural, optical and electrical properties of $\beta$ -rhombohedral boron\*

U. Kuhlmann, H. Werheit\*\* and T. Dose

*Solid State Physics Laboratory, University of Duisburg, D 4100 Duisburg 1 (Germany)*

T. Lundström

*Institute of Chemistry, University of Uppsala, Uppsala (Sweden)*

(Received January 8, 1992)

### Abstract

A systematical investigation of a series of interstitially doped B:Fe solid solutions of the  $\beta$ -rhombohedral boron structure with compositions up to  $\text{FeB}_{29.5}$ , which is close to the maximum solubility, is presented. At an iron concentration of about 2.5% the conductivity character changes from the p-type behaviour of pure  $\beta$ -rhombohedral boron to n-type. The IR and Raman active phonons change systematically. The damping  $\parallel c$  is much stronger than  $\perp c$ . In the case of the stretching mode of the central boron atom in the unit cell, occupied and unoccupied unit cells can be distinguished. An additional splitting of this vibration coincides with the formation of magnetic clusters and the sign reversal of the Seebeck coefficient. Some low frequency absorption bands are attributed to atoms in the definite voids of the structure. The question of whether they are local vibrational modes or electronic transitions remains unsolved. The iron atoms lead to an electronic level at 0.133 eV above the Jahn–Teller induced split-off valence band of  $\beta$ -rhombohedral boron.

### 1. Introduction

The crystal structures of the boron-rich solids contain  $\text{B}_{12}$  icosahedra as their essential common elements. These icosahedra are linked amongst themselves and with other structure elements, *e.g.* different polyhedra or single atoms, by preferably covalent bonds. In the relatively open structures, *e.g.* in  $\beta$ -rhombohedral boron there remain voids of sufficient size to allow the accommodation of transition metal atoms, thus forming solid solutions [1]. The occupation of the different voids depends on the kind, size and amount of foreign atoms dissolved [2–4].

With regard to the application of these boron-rich solids, this interstitial doping is particularly important because the B:Fe solid solution with the nominal composition  $\text{FeB}_{29.5}$  was the first definitely doped n-type  $\beta$ -rhombohedral boron and even the first definitely doped boron-rich solid in general

---

\*Partly presented at the Tenth International Conference on Solid Compounds of Transition Elements, May 21–25, 1991, Münster, Germany.

\*\*Author to whom correspondence should be addressed.

[5]. Meanwhile some other elements have been found that allow the creation of n-type  $\beta$ -rhombohedral boron by interstitial doping [3]. The Jahn–Teller effect acting on the  $B_{12}$  icosahedra was proved to be the essential reason for the p-type character of the pure icosahedral boron-rich solids. The effect forms a split-off valence band that is partially occupied by electrons and correspondingly exhibits an acceptor-like influence on the electronic properties [6–8]. Therefore n-type doping of these semiconductors requires the overcompensation of the unoccupied sites in this split-off valence band.

The results of magnetic investigations on B:Fe solid solutions were interpreted by antiferromagnetic interactions between the soluted iron atoms, and by the formation of magnetic clusters at higher concentrations of iron atoms [9]. Similar results were found in B:Mn [10].

In this study, the influence of the iron atoms and their clustering on the structure of  $\beta$ -rhombohedral boron is investigated on a series of B:Fe specimens with metal concentrations up to the maximum reachable occupancy of interstitial sites. The structure-related spectra of IR and Raman active phonons are presented together with optical absorption spectra in the edge range and the results of the Seebeck coefficient measurements giving information on the electronic states and the conductivity type.

## 2. Specimens

Specimens of the nominal chemical compositions  $FeB_{1080}$ ,  $FeB_{300}$ ,  $FeB_{110}$ ,  $FeB_{40}$ ,  $FeB_{39.5}$  and  $FeB_{29.5}$  were prepared by arc melting and heat treating in BN crucibles at 1470 K for 20 h to guarantee homogeneity. The ingredients were high-purity boron (claimed purity 99.995%; Wacker, Munich) in the case of  $FeB_{29.5}$ , technical boron (claimed purity 99.8%; analysed purity 99.4% with 0.3% Fe and 0.1% Si, H.C. Starck, Goslar) for the other specimens and iron (specpure, Johnson Matthey). For more details see refs. 1, 5 and 9.

The essential difference between the types of boron is the carbon concentration, which is typically 50–100 ppm in Wacker boron and about 0.1–0.2% in Starck boron. In most of the results presented in this study the influence of iron atoms on properties will be shown to be overwhelming. Otherwise the influence of the different carbon contents will be discussed in connection with the individual results.

## 3. Structure

In the presentation of the unit cell of  $\beta$ -rhombohedral boron, outlined in Fig. 1, the different voids able to accommodate foreign atoms are outstanding [4]. In the case of B:Fe, only the sites A(1) (Me 1) and D (Me 2) are relevant.

The occupancies of these voids were derived from electron density determinations [1, 2, 11]. As shown in Fig. 2, they both increase linearly with the iron content, but the occupancy of the A(1) position is three times

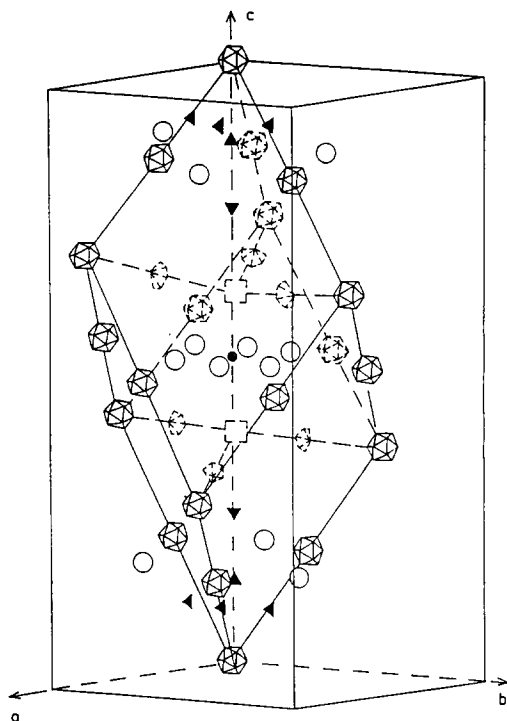


Fig. 1. Unit cell of  $\beta$ -rhombohedral boron with  $B_{12}$  icosahedra,  $B_8$  half-icosahedra,  $B_{10}$  subunits (squares), the central B atom (B 15), the A(1) (Me 1), D (Me 2), E (Me 3) and Si(2) positions.

Symbol	Designation	Coordinates			Position
▲	A (1), Me 1	0	0	0.135	6 c
○	D, Me 2	0.245	0.41	0.17	36 i
▼	E, Me 3	0	0	0.245	6 c
◄	Si (2)	0.11	0.89	0.10	18 h
●	B 15	0	0	0.5	3 b

as high as that of the D position. Since there are only two crystallographically equivalent A(1) positions in comparison with six equivalent D positions, the numbers of iron atoms on the A(1) and D sites per unit cell are obviously the same throughout the whole doping range. This is contrary to the assumption of Tsiskarishvili *et al.* [9] who assumed a preferential occupation of the A(1) sites. Based on 106.7 B atoms in the unit cell of  $\beta$ -rhombohedral boron [3] the maximum iron content in  $\beta$ -rhombohedral boron is apparently reached in  $FeB_{26.6}$ , which is in a quite good agreement with the solubility investigations. This corresponds to four iron atoms per unit cell from which, according to Fig. 2, there are two on the A(1) site and two on the D site. While the A(1) sites are therefore completely occupied, the six D sites accommodate only two iron atoms. Since this situation corresponds to the maximum occupancy

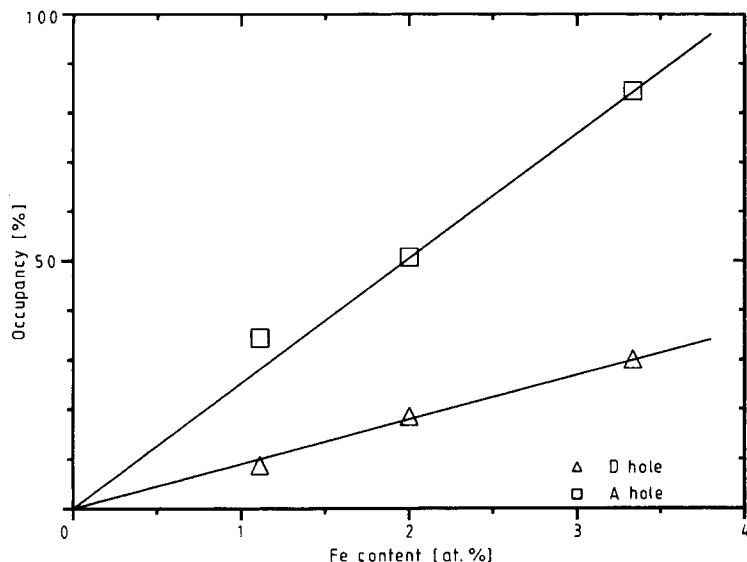


Fig. 2. Occupancies of the A (Me 1) and the D (Me 2) interstitial holes in B:Fe solid solutions [2, 3, 11].

for the D sites, the assumption of a diametral arrangement of both iron atoms in a distance of 4.85 Å bridged by the central B(15) atom in the unit cell seems to be the only convincing one. This is contrary to ref. 9, where closer arrangements of the iron atoms are considered. These would lead to a maximum occupancy of three respectively four iron atoms in the D sites of the rhombohedral unit cell, in contrast to the experimental results. The six radially distributed D sites allow three such orientations of two iron atoms. Whether there is a statistical or co-linear orientation of these arrangements in different unit cells cannot be determined from the structural data of polycrystalline material presently available (see the discussion of the low frequency absorption bands below). From the isotropic position distribution of the B(15) atom  $\perp c$  in B:Al [12] it can be concluded that, in this case, the orientation is statistical, but this is not necessarily valid in the case of iron and manganese atoms because of their possible magnetic exchange interaction.

The unit cell dimensions depending on the iron content obtained with a Guinier-Hägg camera [2, 4, 5] are shown in Fig. 3 and seem to vary proportionally to the iron content within the accuracy of the measurements. The maximum distortions in  $\beta$ -rhombohedral boron saturated with iron amounted to 0.35% for the  $c$  axis and 0.56% for the  $a$  axis. To rate the data in Fig. 3 at lower occupancies, it must be remembered that they are obtained by averaging a large number of unit cells, that are only statistically occupied by iron atoms. Therefore, the real distortions of the individual unit cells with occupied interstitial sites may be as large as the value derived for the maximum occupation, while unoccupied unit cells remain largely

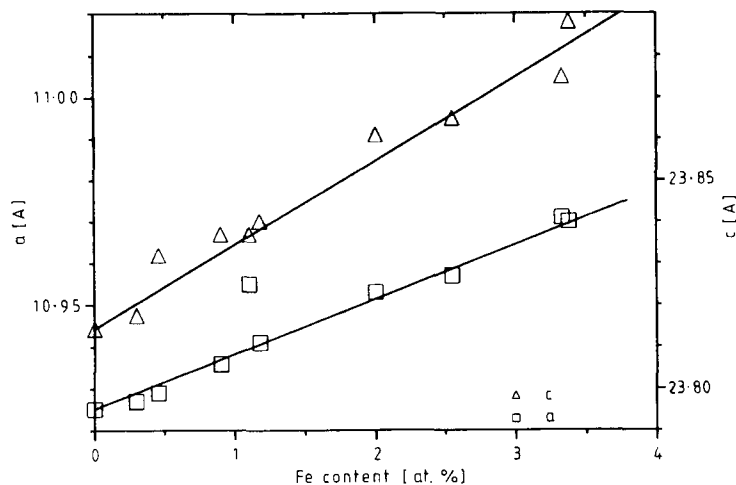


Fig. 3. Unit cell dimensions of B:Fe solid solutions. Data from this work and from refs. 2, 3, 5 and 11.

undistorted. This leads to considerable structure fluctuations throughout the crystal.

From Fig. 3 the relation of the relative elongations

$$\Delta a/a:\Delta c/c=1.59(6)$$

is calculated, but this value must be revised if a statistical distribution of the linearly aligned iron pairs on the D sites is assumed. Then the weight factor of the averaged relative linear distortion of the  $a$  axis is 0.667 leading to

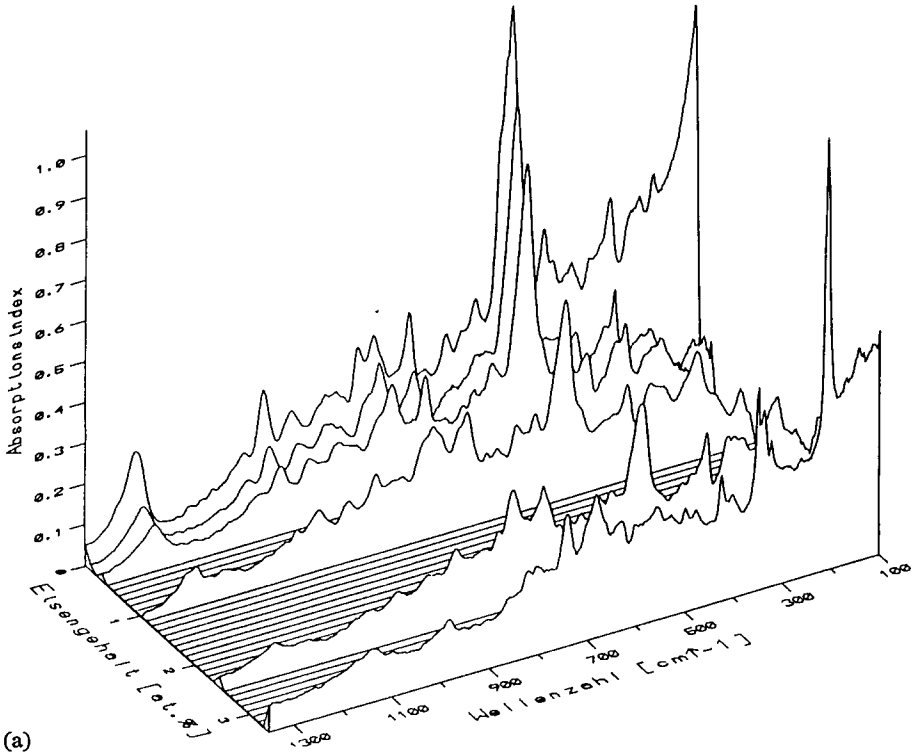
$$\Delta a/a:\Delta c/c=2.38(8)$$

for the maximum distortion of the  $a$  axis parallel to the direction in which both iron atoms on the D sites are accommodated. In any case, the distortion  $\perp c$  is considerably stronger than for  $\parallel c$ , which seems to lead to the conclusion that the bonding forces in the A voids are distinctly stronger than those in the D voids.

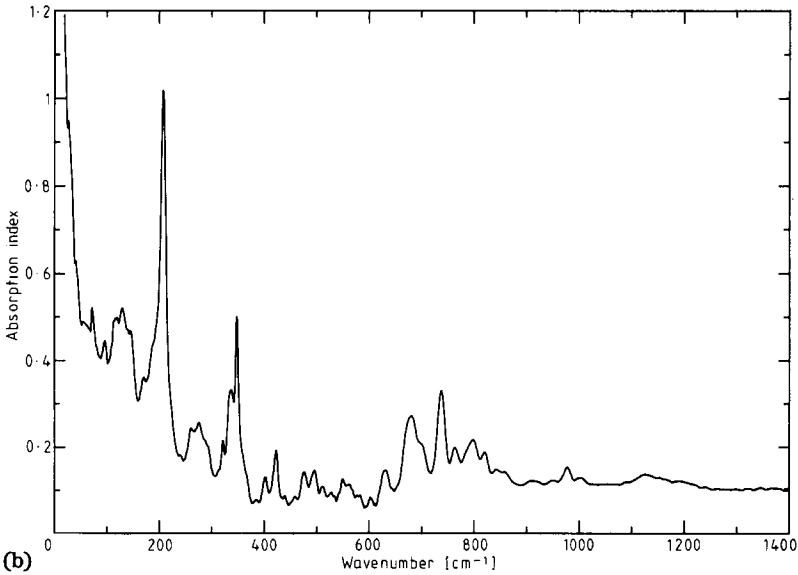
## 4. Lattice vibrations

### 4.1. IR active phonons

The IR spectra were obtained at room temperature with a FTIR spectrometer IFS 113v (Bruker, Karlsruhe). The reflectivity was measured on polished surfaces and the data mathematically transferred to the absorption index by a Kramers–Kronig transformation. The spectra are shown in Fig. 4. In the case of pure  $\beta$ -rhombohedral boron, the spectrum at low wave numbers ( $<250\text{ cm}^{-1}$ ) is influenced by the reflection from the back surface of the plane-parallel sample because of the low absorption of  $\beta$ -rhombohedral boron in this spectral range [13]. This means that the increase of the



(a)



(b)

Fig. 4. (a) 3-dimensional plot of the absorption spectra of B:Fe ( $\text{FeB}_{1080}$ ,  $\text{FeB}_{300}$ ,  $\text{FeB}_{100}$ ,  $\text{FeB}_{40}$ ,  $\text{FeB}_{39.8}$ ,  $\text{FeB}_{29.5}$ ) vs. Fe content compared with high purity  $\beta$ -rhombohedral boron. In the case of pure  $\beta$ -rhombohedral boron the  $k$  values increasing towards low wave numbers are simulated by the back surface reflexion of the plane parallel sample and therefore are not real. (b) Absorption index of  $\text{FeB}_{29.5}$  vs., wave number.

absorption in this range towards low wave numbers is largely simulated. In the case of the iron-doped samples, the back surfaces were not parallel to the front surfaces, and therefore their increasing reflectivity towards low photon energies is real.

There are three frequency ranges of the spectra to be distinguished.

#### 4.1.1. The stretching vibration of the central atom in the unit cell [13] (at about $1250\text{ cm}^{-1}$ )

As in B:Mn even at very low metal concentrations [4] a vibration, which is additional to the normal one, is found to shift to a somewhat lower frequency (Fig. 5). This is obviously due to the modified restoring forces acting on the central atoms in unit cells where interstitial sites are occupied. Moreover at a certain higher concentration of interstitial iron atoms, a considerable additional shift of both vibration frequencies is seen which coincides with the assumed formation of long-range magnetic clusters also seen in B:Mn [9, 10].

The broadening of this additional stretching vibration band with increasing iron content can be partly attributed to the strong damping  $\parallel c$  (see 4.1.2). Alternatively, there may be an influence of less-defined restoring forces in unit cells with partly occupied A(1) and D sites.

#### 4.1.2. Intraicosahedral vibrations (at about $650\text{--}1050\text{ cm}^{-1}$ )

In accordance with a number of experimental and theoretical results, the phonons of this range can be attributed to the intraicosahedral vibrations [4]. Since polycrystalline samples are investigated in this study, both crystalline

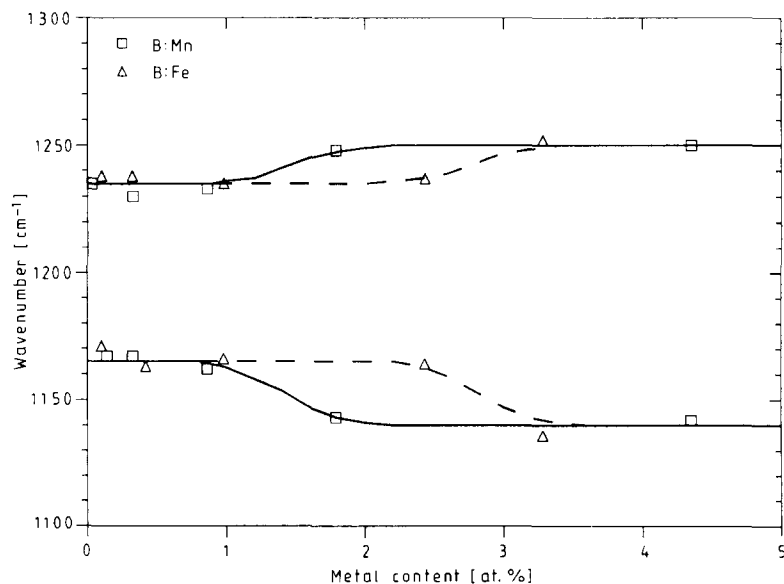


Fig. 5. Stretching vibration mode of the central atom in the unit cell of  $\beta$ -rhombohedral boron (B 15) and its variations with the iron content increasing in comparison with B:Mn [4].

orientations contribute to the measured phonon spectra and the modifications induced by the metal atoms can essentially be estimated only from the variations of the prominent peaks. The result is that the vibrations of the type  $A_{2u}$  ( $E \parallel c$ ) are considerably damped with increasing iron content, while the vibrations of the type  $E_u$  ( $E \perp c$ ) remain largely unchanged. This can be clearly seen in the spectrum of  $FeB_{29.5}$ , which is similar to the  $E_u$  spectrum ( $E \perp c$ ) of pure  $\beta$ -rhombohedral boron in this spectral range (compare refs. 12 and 14). Undoubtedly, the damping is also influenced by the carbon content of the samples. However, because of the systematical variation depending on the iron content, this is not essential for the following interpretation. Particularly, in the case of  $FeB_{29.5}$  prepared from high purity boron.

The reason for this anisotropic damping cannot be the anisotropic structure variation caused by the iron atoms, because it was shown above that the relative distortion  $\perp c$  exceeds  $\parallel c$  considerably. From the structure it can be seen that the A(1) site on the main diagonal of the unit cell is an immediate neighbour to the icosahedron at the vertex of the unit cell. It therefore seems plausible that it hinders its movement in this direction.

This result is important to the discussion about the origin of the intraicosahedral vibrations of  $\beta$ -rhombohedral boron in this range; are they owing to split  $F_{1u}$  modes of the isolated icosahedron resulting from a resonance coupling of the different icosahedra in the unit cell or owing to the IR active vibration modes of the icosahedron in the  $D_{3d}$  symmetry of the structure becoming active in both directions ( $\parallel c$  and  $\perp c$ ) by symmetry reductions in the structure (compare discussion and Table 5 in ref.4)? Since the iron atoms in the A(1) position can only be assumed to influence the vibration modes  $\parallel c$  of the icosahedron at the vertex of the unit cell, but not of those on its edges, especially not their vibrations  $\parallel c$ , the present result seems to support the second model of interpretation.

*4.1.3. Intraicosahedral vibrations (at about 150–600  $cm^{-1}$ ) and low frequency absorption bands due to the iron atoms (<500  $cm^{-1}$ )*

The vibrations of the rigid icosahedra and other big structure elements of the unit cell are attributed to a spectral range of about 150 and 600  $cm^{-1}$  [4]. They are damped when the iron content increases because the long-range order of the crystal is progressively disturbed. The reason being the structure fluctuations in the consequence of the statistically distorted unit cells described above.

The new significant absorption bands which grow from the background of the intraicosahedral vibrations as the iron content increases become prominent in the spectrum of  $FeB_{29.5}$ . This seems to indicate that a long-range order to occupied interstitial sites is a prerequisite of the assumption that the formation of magnetic clusters is related to the formation of these absorption bands.

According to present knowledge, two different models seems to explain the origin of these bands. One model attributes them to local vibrations of



the metal atoms in the different voids. In comparison with the optical spectra of other solid solutions of  $\beta$ -rhombohedral boron [4], some of these vibrations can be attributed to one another and to definite voids, as shown in Fig. 6. The frequencies are plotted *vs.* (atomic weight)<sup>-1/2</sup> to consider the influence of the different masses of the atoms. The non-linear behaviour indicates that the restoring forces acting on the metal atoms in the voids depend on the kind of metal atoms. The number of electrons in the outermost orbitals of the metal atoms (Cu: 4s<sup>1</sup>; Fe, Mn; 4s<sup>2</sup>; Al: 3s<sup>1</sup>) are obviously not sufficient to explain the different bond strengths, but if the electrons are transferred to the boron framework, leading to a certain ionicity of the bonds, this would be more relevant.

The peak at 200 cm<sup>-1</sup> (B:Fe) is assigned to the void A(1) because this absorption is found only in solid solutions in which this void is occupied. For the same reason the occupation of site A(1) is assumed to be responsible for damping the strong phonon band at 480 cm<sup>-1</sup>.

The absorption band at about 320 cm<sup>-1</sup> (B:Fe) is assigned to void D for several reasons. The occurrence of this band in B:Mn and B:Fe is correlated with the actual occupation density, which is high in the case of manganese even at low metal concentrations, but only becomes appreciable in B:Fe at high doping levels. Moreover, according to crystallographic investigations [4], the site is a twofold split in B:Cu and a threefold split in B:Cu/Al in agreement with the splitting of the absorption bands (in Cu/Al even a fourfold splitting of this site seems possible according to the spectrum). If this assignment is correct, according to the spectra a threefold splitting should exist in the case of B:Fe and a twofold splitting in the case of Mn. This

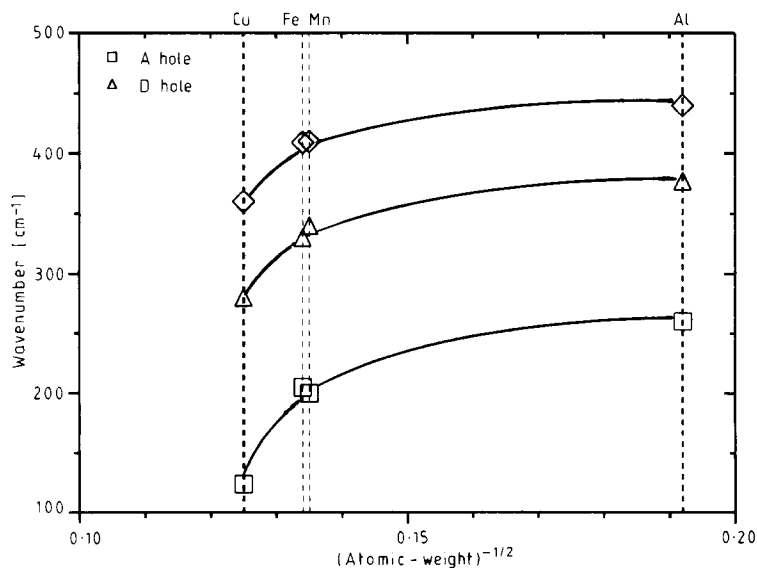


Fig. 6. Several low frequency absorption frequencies of transition metal solid solutions of  $\beta$ -rhombohedral boron plotted *versus*  $1/(\text{at.wt.})^{-1/2}$ .

has not yet been detected crystallographically. With respect to B:Fe the discussion in the previous section on the structure is recalled, in which three different orientations of iron pairs are possible that, at first, are expected to be degenerated. Because of the anisotropic distortions of the unit cell, three slightly different restoring forces seem possible in agreement with the splitting of the phonon absorption band.

The relation of the restoring forces attributed to the three peaks of the  $320\text{ cm}^{-1}$  absorption can be roughly estimated from the spectral positions according to a simple relation  $k \sim f^2$  leading to 1:0.935:0.85. The corresponding absorption intensities are approximated in the relation 3:2:1.

When these absorption peaks represent local vibrations, their intensities are proportional to the number of iron atoms bonded under the related conditions. The strongest absorption peak of this threefold split vibration is to be attributed to the highest restoring force. This is expected to belong to the direction of the strongest distortion parallel to the orientation of the iron pair and be additionally influenced by the distortion of the neighbouring unit cells. Therefore a parallel orientation of the iron pairs arranged in the D sites of the different unit cells of the crystal seems to be distinctly more probable than a statistical orientation.

A weaker twofold split band is seen at  $410\text{ cm}^{-1}$  (B:Fe). The corresponding band in B:Mn is single, while those in B:Cu and B:Cu/Al are twofold [4]. At present there are no corresponding indications in the crystallographic results. The E hole can be excluded from this explanation, because this site is occupied in B:Mn and B:Cu, but not in B:Fe and B:Cu/Al.

The occupation of the E void seems to influence the sharpness of the absorption bands of the interstitial metal atoms. It is occupied in B:Mn and B:Cu, where these low frequency bands are broad (which means that they are considerably damped) and unoccupied in B:Fe and B:Cu/Al, in whose spectra the bands are only very weakly damped.

A different possibility to explain these low frequency absorption bands in interstitially doped  $\beta$ -rhombohedral boron could be their attribution to electronic transitions. A support for such an assumption is their low halfwidth compared with the phonon bands even in pure  $\beta$ -rhombohedral boron, especially when the rather large thermal vibration ellipsoid of interstitial metal atoms is considered [15]. Similar FIR absorption peaks, which were attributed to electronic transitions were found in  $\text{MgO}:\text{Co}^{2+}$  [16] and  $\text{MgO}:\text{Fe}^{2+}$  [17]. Their energetical position is in a fairly good agreement with the splitting energies of the electronic levels of the metal atoms expected in the case of a tetrahedral crystal field probably modified by the Jahn–Teller effect [18].

In this respect, the ionisation degree of the interstitially accommodated metal atoms is important, as is their interaction with the local crystal field which determines the splitting of the electronic levels. The surrounding of the A site in  $\beta$ -rhombohedral boron is approximately tetrahedral, while that of the D site, surrounded by 15 B atoms with distances varying between 2.01 and 2.45 Å, is much more complex. The electron spin resonance (ESR) spectra have been controversially discussed. While Tsiskarishvili *et al.* [9,

10] try to attribute the ESR spectra of B:Fe and B:Mn to twofold and threefold ionized metal atoms, Klein and Geist [19] showed that the ESR spectrum of B:Mn can be interpreted by the assumption of neutral metal atoms, whose 4s electrons are transferred to 3d states. This would be in accordance with the findings of Ludwig and Woodbury [20] on interstitial transition metal atoms in silicon. The question of whether the FIR absorption bands in  $\beta$ -rhombohedral boron are of vibrational or electronic nature needs further investigation.

#### 4.2. Raman active phonons

The Raman-active phonon spectra of the B:Fe solid solutions were measured with a FT Raman spectrometer (Bruker, Karlsruhe). Some characteristic qualitative results are shown in Fig. 6. Raman-active phonon spectra are much more sensitive to structure distortions than IR-active phonon spectra; therefore the essential information, which can be derived from the spectra with respect to the influence of the iron atoms, is that the structures are distorted. This is in agreement with the structure discussion in the corresponding section of this paper. Besides the distortion caused by iron, the carbon impurities also have an essential influence. This can be obtained by comparing the Raman spectrum of Starck boron without additional iron doping with the spectrum of Wacker boron. Nevertheless, it can be seen that the structure distortions induced by the iron atoms are considerably stronger than those of the carbon atoms. Again it should be taken into consideration that  $\text{FeB}_{29.5}$  was prepared from high purity boron.

### 5. Electronic transitions

As mentioned in the introduction, the conductivity type of  $\beta$ -rhombohedral boron can be changed by an overcompensation of vacant electronic states in the split-off valence band. To find out where the energetical position of the iron atoms is in the band gap, optical absorption measurements in the spectral range of the absorption edge were performed. Figures 7 and 8 show the spectra of  $\text{FeB}_{300}$  and  $\text{FeB}_{1080}$  and the calculated difference spectrum. Since both specimens were prepared from boron of the same origin, the influence of other impurities on the absorption spectrum can be largely eliminated by this procedure. This can especially be seen at the absorption peak at 0.277 eV, which is attributed to carbon in  $\beta$ -rhombohedral boron.

The selection of the best fit to an absorption theory yields an indirect (probably non-direct) allowed interband transition with the minimum transition energy of

$$\Delta E = 0.133(5) \text{ eV}$$

There is probably a second transition at 0.64(2) eV, but its verification demands additional measurements towards higher photon energies with thinner samples.

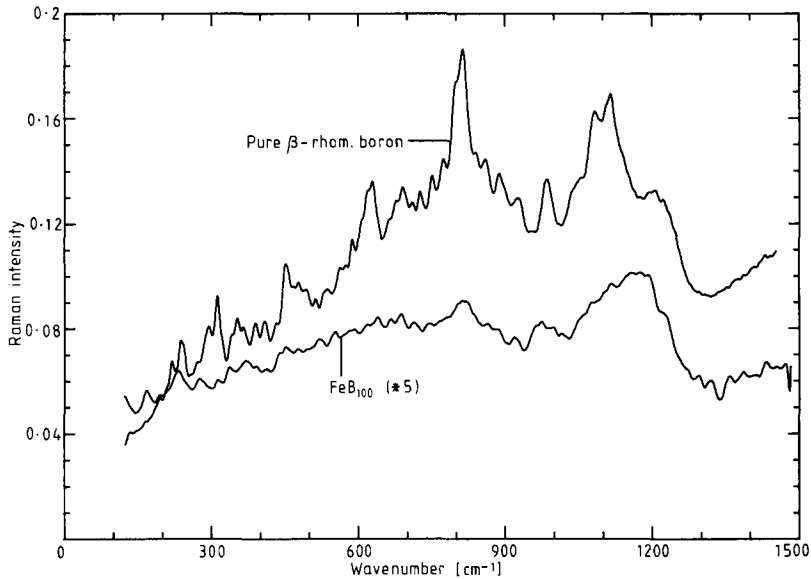


Fig. 7. Typical Raman spectrum (relative intensity) of a B:Fe solid solution in comparison with high purity  $\beta$ -rhombohedral boron.

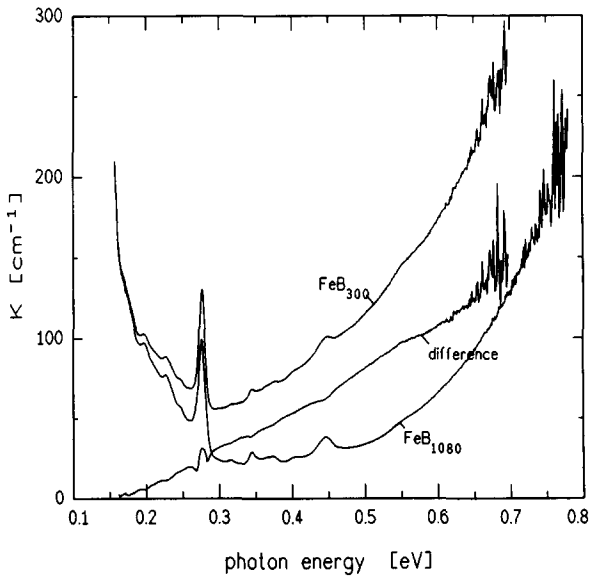


Fig. 8. Optical absorption spectra (absorption coefficient  $K$  vs. photon energy) in the absorption edge tail of  $\text{FeB}_{1080}$  and  $\text{FeB}_{300}$ , and the calculated difference spectrum.

Thus, the iron atoms lead to an energy level at 0.133 eV above the Fermi level, which is positioned within the split-off upper valence band in  $\beta$ -rhombohedral boron at doping concentrations below the compensation limit.

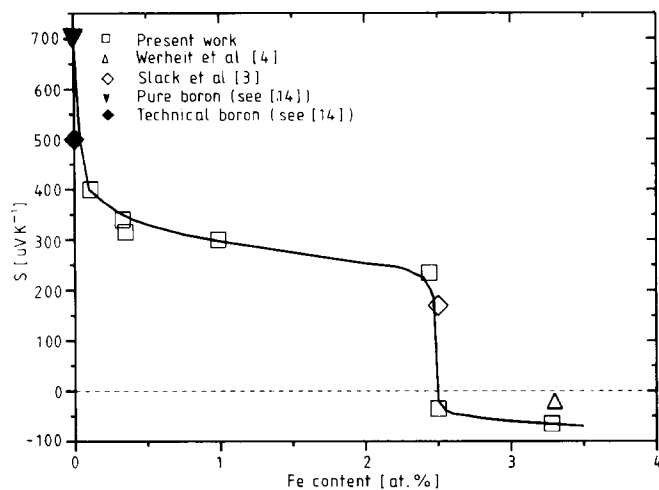


Fig. 9. Seebeck coefficient of B:Fe at 300 K in comparison with the corresponding data obtained on high purity boron and technical boron.

## 6. Seebeck coefficient

The transport mechanism in  $\beta$ -rhombohedral boron is determined by hopping processes in pure and highly iron-doped material [5, 14, 21]. Therefore the Hall effect is not a reliable method of determining the conductivity character of these materials. To obtain the change of the conductivity character of  $\beta$ -rhombohedral boron throughout the range of the iron doping, the Seebeck coefficient was measured on the materials that were at our disposal. Figure 9 shows the results in comparison with those of high purity, of carbon contaminated, and of iron-doped  $\beta$ -rhombohedral boron obtained from the literature.

The sign reversal of the Seebeck coefficient *i.e.* the compensation of the unoccupied sites in the upper valence band, takes place at an iron content of 2.5 at%. This coincides with the cluster formation ([9] and Fig. 5). But, contrary to B:Fe, B:Mn remains p-type throughout the whole range of doping, including the range of magnetic cluster formation, so the magnetic clusters cannot be the reason for the sign reversal of the carriers in  $\beta$ -rhombohedral boron.

According to Mott and Davis [22], the quantity of the Seebeck coefficient is determined by the gradient of the density of states at the Fermi level. Therefore, from Fig. 9, the qualitative distribution of the density of states in the upper region of the split-off upper valence band can be estimated.

## Acknowledgement

The investigations were partly supported by the Minister of Research and technology of the Federal Republic of Germany under contract number 317-4003-0328845A.

## References

- 1 T. Lundström, Solid solutions and metal borides based on icosahedral arrangements of the boron atoms, in H. Werheit (ed.), *Proc. Int. Symp. Boron, Borides and Related Compounds, September 21–25*, University of Duisburg, 1987, p. 53.
- 2 B. Callmer and T. Lundström, *Solid State Chem.*, **17** (1976) 165.
- 3 G. A. Slack, J. H. Rosolowski, C. Hejna, M. Garbaskas and J. S. Kasper; in H. Werheit (ed.), *Proc. 9th Int. Symp. Boron, Borides and related Compounds*, University of Duisburg, September 21–25, 1987, p. 132.
- 4 H. Werheit, H. Haupt, T. Lundström and I. Higashi, *Z. Naturforsch.*, **45a**, (1990) 101.
- 5 H. Werheit, K. de Groot, W. Malkemper and T. Lundström, *J. Less-Common Met.*, **82** (1981) 163.
- 6 R. Franz and H. Werheit, *Europhys. Lett.*, **9** (1989) 145.
- 7 R. Franz and H. Werheit, Influence of the Jahn–Teller effect on the electronic band structure of boron-rich solids containing B<sub>12</sub> icosahedra, in D. Emin, T. L. Aselage, A. C. Switendick, B. Morosin and C. L. Beckel (eds.), *Proc. 9th Int. Symp. Boron, Borides and related Compounds, Albuquerque, NM, 1990, CHIP Conf. Proc. 23rd*, American Institute of Physics, NY, p. 29.
- 8 H. Werheit, On the electronic transport properties of boron carbides, in R. Freer (ed.), *The Physics and Chemistry of Carbides, Nitrides and Borides*, Kluwer, Dordrecht, 1990, p. 677.
- 9 G. P. Tsiskarishvili, T. Lundström, L. Lundgren, G. V. Tsagareishvili, O. A. Tsagareishvili and F. N. Tavadze, *J. Less-common Met.*, **142** (1988) 91.
- 10 G. P. Tsiskarishvili, T. Lundström, L. Lundgren, G. V. Tsagareishvili, D. N. Tsikaridze and F. N. Tavadze, *J. Less-Common Met.*, **147** (1989) 41.
- 11 R. E. Hughes and L. T. Tai, personnel communication, 1973.
- 12 I. Higashi, M. Kobayashi and Y. Akagawa, in D. Emin, T. Aselage, C. L. Beckel, I. A. Howard and C. Wood (eds.), *Boron-rich Solids (AIP Conference Proceedings 140) Albuquerque, NM, 1985*, American Institute of Physics, p. 224.
- 13 H. Binnenbruck and H. Werheit, *Z. Naturforsch.*, **34a** (1979) 787.
- 14 H. Werheit, Boron, in O. Madelung, M. Schulz and H. Weiss (eds.), *Landoldt–Börnstein Numerical Data and Functional Relationships in Science and Technology (New Series) Vol. III/17e*, Physics of Non-Tetrahedrally Bonded Elements and Binary Compounds I, Springer, Berlin, 1983, p. 9.
- 15 T. Lundström, in D. Emin, T. Aselage, C. L. Beckel, I. A. Howard and C. Wood (eds.), *Boron-Rich Solids, (AIP Conference Proc. 140)*, Albuquerque, NM, 1985, p. 19.
- 16 W. Low, *Phys. Rev.*, **109** (1985) 256.
- 17 J. Y. Wong, *Phys. Rev.*, **168** (1968) 337.
- 18 F. S. Ham, Jahn–Teller effects in electron paramagnetic resonance spectra, in S. Geschwind (ed.), *Electron Paramagnetic Resonance*, Plenum, New York, 1972, p. 1.
- 19 W. Klein and D. Geist, *Z. Phys.*, **201** (1967) 401.
- 20 G. W. Ludwig and H. H. Woodbury, Electron spin resonance in semiconductors, *Solid State Physics*, **13** (1962) 223.
- 21 H. Werheit, Boron compounds, in O. Madelung, M. Schulz and H. Weiss (eds.), *Landoldt–Börnstein, (New Series) Vol. 17g*, Springer, Berlin, 1983, p. 9.
- 22 N. F. Mott and E. A. Davis, *Electronic Processes in Disordered Materials*, Clarendon Press, Oxford, 1979.